Comparison of the Failures during Cyclic Oxidation of Yttria-Stabilized (7 to 8 Weight Percent) Zirconia Thermal Barrier Coatings Fabricated *via* Electron Beam Physical Vapor Deposition and Air Plasma Spray

N.M. YANAR, M. HELMINIAK, G.H. MEIER, and F.S. PETTIT

The failures during oxidation of electron beam physical vapor deposition (EBPVD) and air plasma spray (APS) yttria-stabilized zirconia (YSZ) thermal barrier coatings (TBCs) on different bond coats, namely, platinum-modified aluminide and NiCoCrAlY, are described. It is shown that oxidation of the bond coats, along with defects existing near the TBC/bond coat interface, plays a very important role in TBC failures. Procedures to improve TBC performance *via* modifying the oxidation characteristics of the bond coats and removing the as-processed defects are discussed. The influence of exposure conditions on TBC lives is described and factors such as cycle frequency and thermal gradients are discussed.

DOI: 10.1007/s11661-010-0436-7

I. INTRODUCTION

THERMAL barrier coatings (TBCs) are widely used to decrease the temperature (~140 K to 170 K (~140 °C to 170 °C)) of metallic hardware used in hot gas environments. Such TBCs usually consist of a ceramic top coat on a metallic bond coat, which in turn is on a metallic alloy. In the case of TBCs used in gas turbines, the ceramic top coat is usually yttria-stabilized (7 to 8 wt pct) zirconia (YSZ). The top coat is fabricated *via* electron beam physical vapor deposition (EBPVD) or air plasma spray (APS) processes. Typical microstructures of YSZ TBCs fabricated *via* EBPVD and APS processes are shown in Figures 1 and 2, respectively. The strain compliance in the EBPVD TBCs is achieved *via* the columnar microstructure with the small openings between the columnar crystallites (Figure 1). The strain tolerance in the APS TBCs results from cracks and voids in the TBCs (Figure 2).

The bond coats upon which the top coats are deposited may be diffusion aluminide coatings or MCrAlY overlay coatings. Very often the diffusion coating contains platinum, and a typical aluminide coating is shown in Figure 3. The MCrAlY bond coats may be NiCoCrAlY (*e.g.*, Ni-22Co-16Cr-13Al-0.5Y wt pct) or some modifications with different amounts of Ni, Co, Cr, and Al. A typical NiCoCrAlY bond coat is shown in Figure 4. The substrates are usually superalloys such as Renè N5 (GE, Evendale, OH) or PWA 1484 (Pratt & Whitney, E. Hartford, CT). As EBPVD TBCs are fabricated, the substrates are at temperatures of approximately 1273 K (1000 °C). Consequently, thin thermally grown oxide (TGO) layers are formed upon the bond coats, and the TGOs grow as the coated hardware is used in practice. A schematic representation of turbine blades with TBC, TGO, bond coat, and substrate is shown in Figure 5. This figure shows the thicknesses of aluminide bond coat and the EBPVD fabricated TBC. The MCrAlY bond coats are usually about 100-μm thick and YSZ TBCs prepared *via* APS can have various thicknesses but usually are at least ~300 μm and in some cases may be greater than 1000 μm.

There are numerous articles that describe TBCs[1–4] and TBC failures.[5–9] A TBC failure mechanism that is common to EBPVD TBCs on heavy grit-blasted platinum-modified aluminides involves rumpling or ratcheting of the coating and the TGO. As discussed by Spitzberg *et al.*[7] during thermal cycling, the TGO undergoes displacement instability with periodic penetrations of the TGO into the bond coat. The downward displacements cause strains in the TBC perpendicular to the TBC-TGO interface and cracks form in the TBC. These cracks (Figure 6) extend laterally and eventually coalesce, resulting in buckling of the TBC.

The rumpling/ratcheting type of failures originates in the vicinity of the TBC/TGO interface. As discussed by Hutchinson and Evans,[10] there are also TBC failures within the thermal barrier layer. These failures consist of vertical separations in the TBC from which cracks develop and propagate laterally through the TBC. These vertical separations in the TBC are connected to the constraint on the thickening of the TGO forming near ridges on the bond coat surface (Figure 7).[11] Since this growth cannot be accommodated, stresses are induced that form and widen the gap.

Gell *et al.*[12] studied TBC failures on as-aluminized platinum-modified aluminide bond coats and proposed

N.M. YANAR, Research Assistant Professor, M. HELMINIAK, Graduate Student, and G.H. MEIER and F.S. PETTIT, Professors, are with the National Energy Technology Laboratory and the Department of Mechanical Engineering and Materials Science, University of Pittsburgh, Pittsburgh, PA 15261. Contact e-mail: nmy4@pitt.edu

Manuscript submitted September 24, 2009.
Article published online November 17, 2010

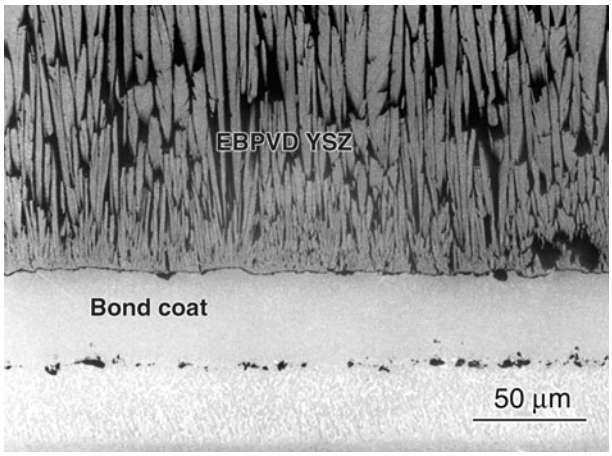

Fig. 1—Scanning electron micrograph showing typical microstructure of an EBPVD YSZ TBC.

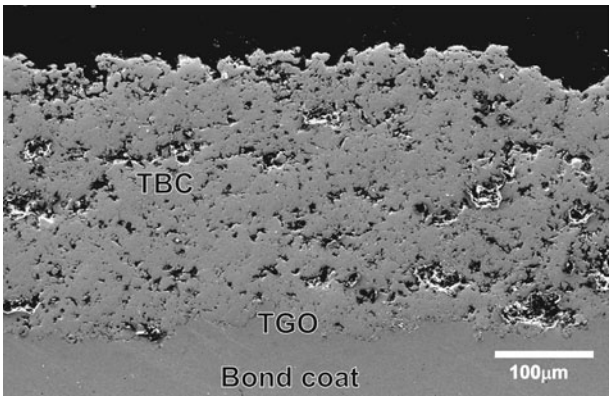

Fig. 2—Scanning electron micrograph showing typical microstructure of an APS YSZ TBC.

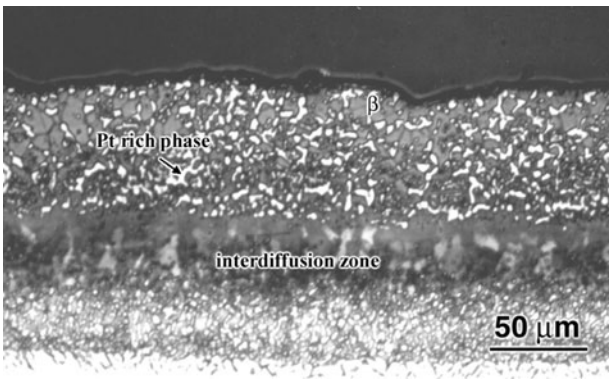

Fig. 3—Micrograph showing an as-processed platinum-modified diffusion aluminide coating. In some platinum-modified aluminides, the platinum-rich phase may not be present and the platinum is in the β phase. These microstructures are dependent upon the thickness of the platinum layer and the aluminizing conditions.

that cracks initiated at bond coat ridges due to out-of-plane tensile stresses formed at the peak of the ridges (Figure 8). These stresses are large enough to cause

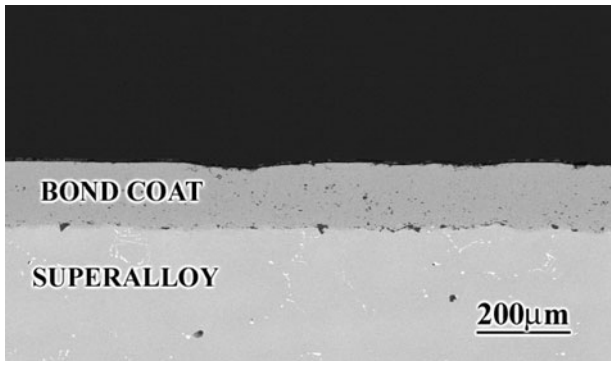

Fig. 4—Micrograph showing an as-processed overlay NiCoCrAlY coating deposited *via* an argon-shrouded plasma spray process.

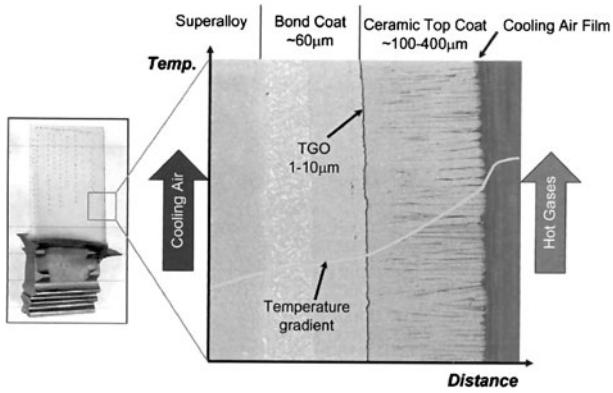

Fig. 5—Example of a cross-sectional image of a TBC system on an aeroturbine blade; the TBC consists of an EBPVD ceramic top coat. Superimposed on the cross-sectional image is the qualitative variation in the temperature across the TBC. The temperature gradient typically is within the range of about 343 K to 423 K (70 °C to 150 °C).

cracking in the TGO above the ridges. The rapid transport of oxygen through these cracks results in preferential oxidation at grain boundaries in the bond coat. Plastic deformation of the bond coat and tensile stresses generated during cooling caused widening of these cracks into cavities and further grain boundary oxidation. This crack and cavity formation around the grain boundary ridges combined with the increase in strain energy as well as the reduction in bond strength along the TGO/bond coat interface resulted in failure of the TBC.

In the case of systems with NiCoCrAlY bond coats, the TGO develops thickness heterogeneities, which contain oxides other than alumina, namely, yttrium-rich oxides such as yttrium aluminum garnet. The magnitude of these heterogeneities, or pegs, is sensitive to the bond coat composition, especially the yttrium content of the coating. Xu *et al.*[13] examined the failure of TBCs on such a system and concluded that these pegs do not seem to be an effective source of the multiple interface cracks needed to create a delamination of the TBC. These authors conclude that delaminations nucleate at large edge imperfections, which, once formed, extend quasi-stably along the interface but cut through the pegs leaving TGO islands embedded in the bond coat (Figure 9). The pegs and edge imperfections

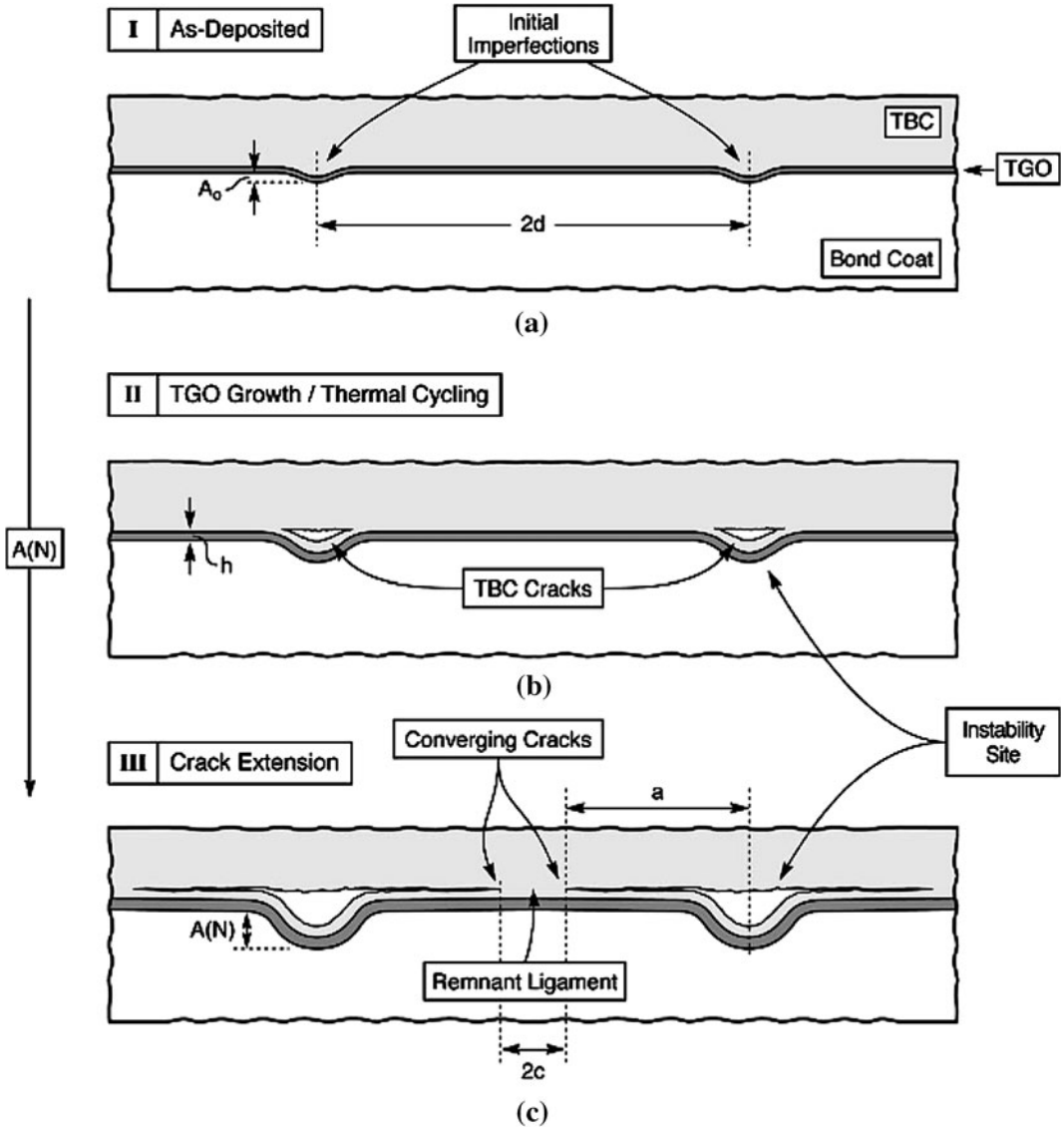

Fig. 6—(*a*) Failure of an EBPVD TBC system driven by a cyclic instability in the thermally grown oxide layer. (*b*) Schematic illustrating the thermomechanical response of (Ni,Pt)Al-based bond coat, indicating the development of a displacement instability. (*c*) The associated crack nucleation and growth in the TBC and crack coalescence leading to coating spallation.[4]

(vertical separations in the TBC) are just two of the many defects that can be present in EBPVD TBCs on NiCoCrAlY bond coats. Other defects can enter into the failure process (*e.g.*, transient oxides in the TGO, an intermixed zone consisting of alumina and zirconia that develops at the TGO-TBC interface).

APS TBCs are deposited on MCrAlY bond coats, and no systems with APS TBCs on platinum-modified aluminide bond coats have been found in the literature. In the case of APS TBCs on NiCoCrAlY bond coats, the bond coat surface is rough (*i.e.*, Ra = 2 μm or greater) in order to develop a mechanical bond between the top coat and the bond coat. It has been shown that failure of plasma-sprayed TBCs occurs within the top coat just above the TGO.[9,14,15] Schlichting *et al.*[8] propose that cracks initiate, as shown in Figure 10, where cracking exists in the TBC and also along the TGO/bond coat interfaces. The primary failure modes in these TBCs appear to be cracking of the bond coat/TGO interface, cracking within the top coat, and linking of these by fracture of the TGO. Rabiei and Evans[9] proposed a similar fracture pattern as that in Figure 10 and emphasized that cracking near the TBC/TGO interface appears to be linked to growth of the TGO in the vicinity of large scale interfacial imperfections. He *et al.*[16] proposed a slightly different cracking pattern, as shown in Figure 11, where TGO growth in conjunction with thermal cycling induces tensile stresses in the TBC normal to the surface. The change in stress with cycling causes cracks to form within the tensile zone between the peaks in the interface oscillations. These cracks penetrate through the islands of compression (Figure 11), where abrupt failure occurs when the energy release rate exceeds the fracture toughness of the TBC.

The TBC failure modes and lives also strongly depend on the exposure conditions. Bolcavage *et al.*[17] compared

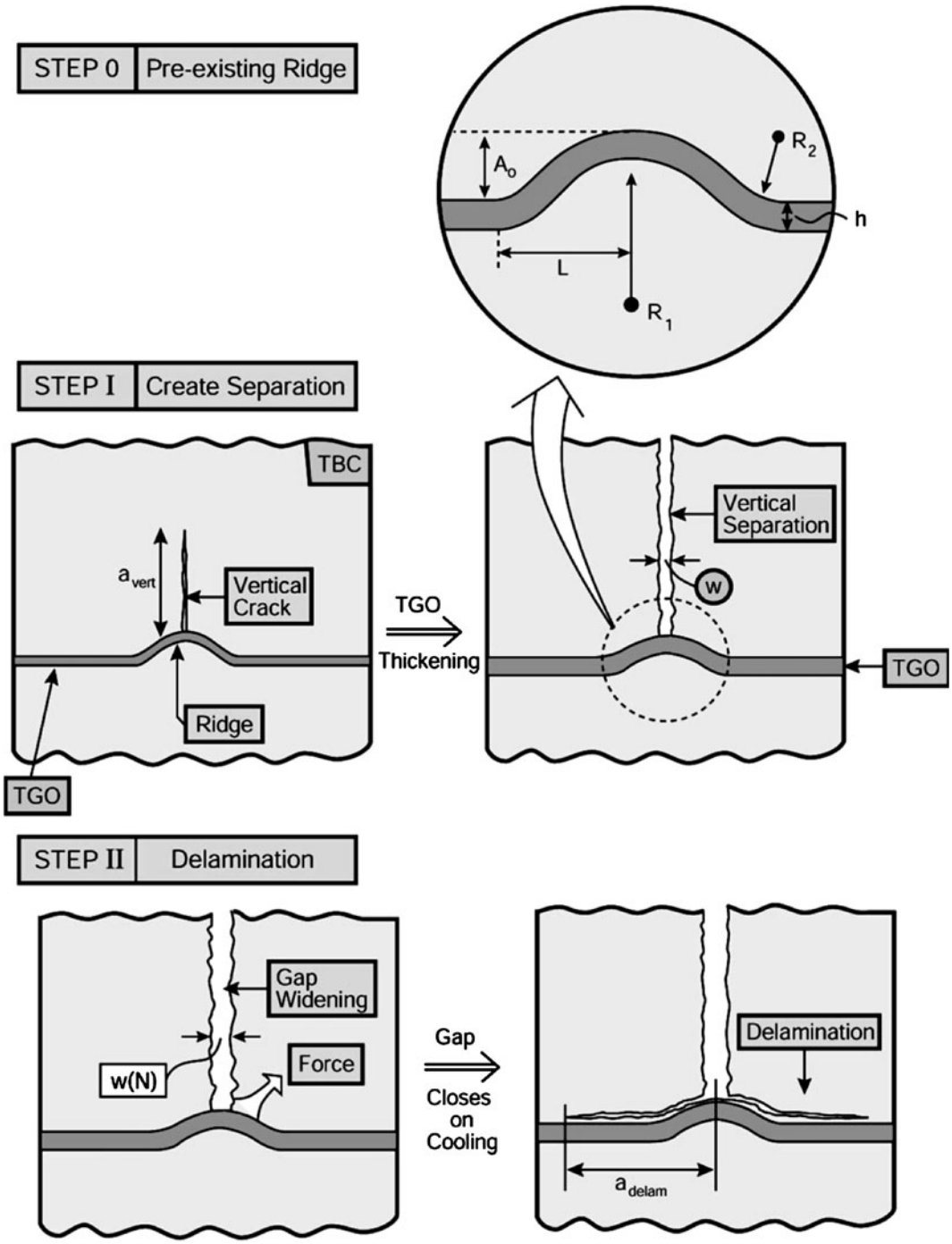

Fig. 7—Schematic illustrating the two stages of delamination. Stage 1: the formation of a vertical separation by TGO formation at ridges in the bond coat. Stage 2: the influence of a vertical separation on delamination (reproduced by permission of 2403770285575).[11]

the behavior of several TBCs exposed in a FCT with those exposed in a "Jet Engine Thermal Simulation" (JETS) test. Bolcavage *et al.*[17] concluded that the FCT test is best suited for those systems in which bond coat oxidation is intimately involved in the failure process (*e.g.*, EBPVD systems), whereas the JETS test is best suited for those systems where fracture in the topcoat is the primary cause of failure (*e.g.*, thick APS TBCs).

Despite numerous articles on TBCs and TBC failures, there are no articles that compare the failures of TBCs fabricated *via* EBPVD and APS. The objectives of this article are as follows:

(1) compare failures of EBPVD and APS YSZ TBCs and present mechanisms for these failures,
(2) discuss modifications of TBCs that can provide longer lives, and
(3) describe the influence of exposure conditions as well as bond coat type and superalloy substrate on these failures.

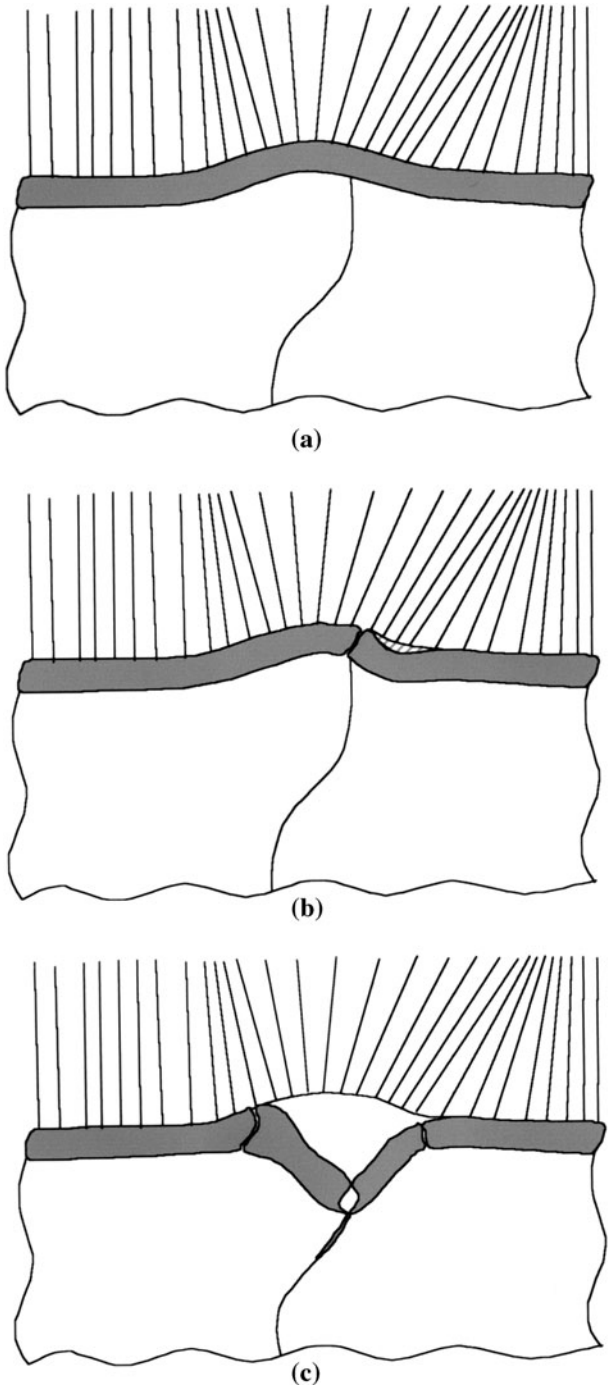

Fig. 8—(*a*) Schematic of thermal cycling mechanism in Pt-Al/EBPVD thermal barrier coatings. Microstructure of an as-received coating showing ridges. (*b*) Cracking of TGO provides a pathway to molecular oxygen and intergranular oxidation. (*c*) Grain boundary cracks widen into cavity and further intergranular oxidation occurs at the base of the cavity (reproduced by permission of 2404300334754).[12]

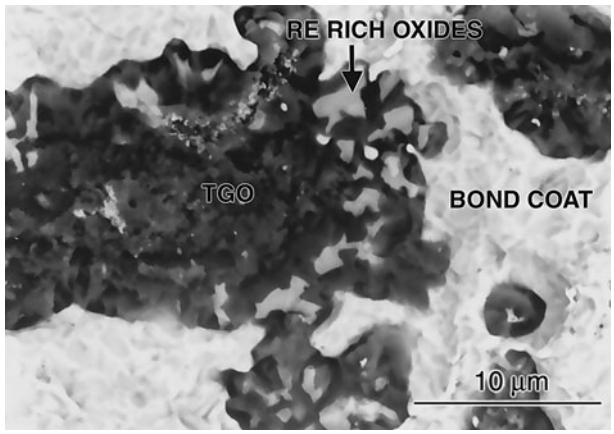

Fig. 9—Scanning electron micrograph from the fracture surface of a NiCoCrAlY bond coat showing delaminations cutting through the pegs leaving TGO islands embedded in the bond coat.

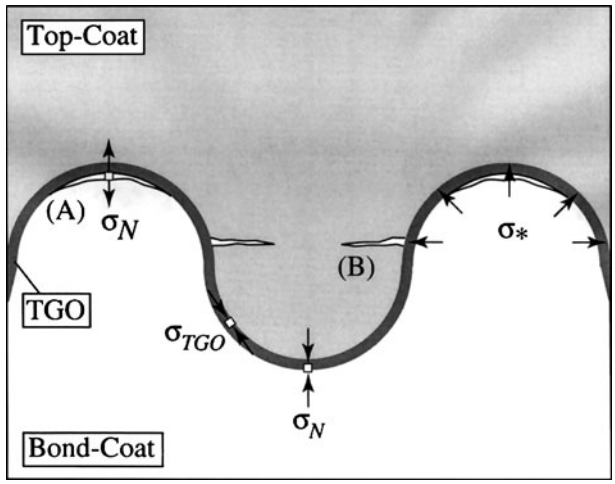

Fig. 10—Schematic diagram depicting the two main types of cracking modes: (*A*) bond coat/TGO cracking driven by σ_N, which is tension at undulation crests and compression at troughs. (*B*) Cracking within the top coat driven by the residual stress, σ^* (reproduced by permission of 2403770444388).[8]

II. EXPERIMENTAL

All experiments were performed using specimens that were circular discs about 2.5 cm (~1 in.) in diameter and 3-mm (0.12-in.) thick. The platinum aluminide bond coats were prepared by electrolytically depositing 5 to 7 μm of platinum on the superalloys and then aluminizing the platinum-coated coupon using a high-temperature, low-aluminum activity diffusion process. The MCrAlY bond coats were deposited on the superalloy substrate using an argon-shrouded plasma spray process. In order to attempt to minimize the defects in EBPVD TBCs on NiCoCrAlY bond coats,[18] the bond coats were polished to Ra ~ 0.3 μm compared to the Ra ~3 μm for the state of the art bond coat surfaces that were initially grit blasted. Also, some bond coats were plated with ~5 μm of platinum and annealed prior to TBC deposition. The YSZ TBCs were prepared by Praxair Surface Technologies (Indianapolis, IN) using EBPVD or APS. The no bond coat TBCs were deposited at two different times in the EBPVD TBC deposition apparatus, and this is identified as first lot and second lot. In addition, some TBCs were deposited on the superalloy after 5 to 7 μm of platinum had been deposited on the superalloy surface and diffused into the

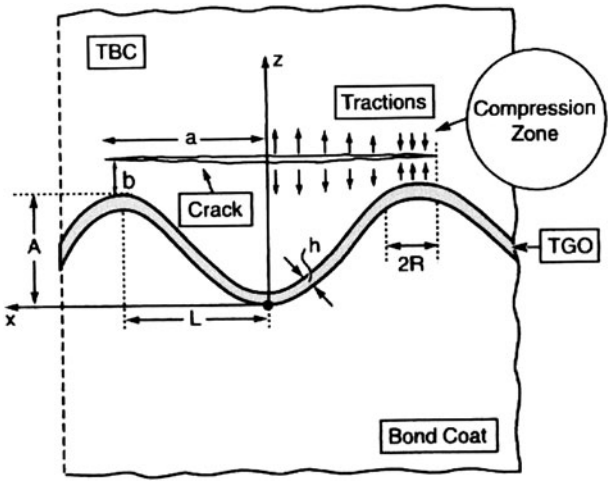

Fig. 11—Schematic of the sinusoidal configuration used for the analysis indicating the location of the cracks in the TBC and the zones of residual tension/compression induced by TGO growth and thermal cycling (reproduced by permission of 2403770549466).[16]

alloy. Some specimens were preoxidized for 50 minutes in air at 1353 K (1080 °C). The APS TBCs were low density (85 pct) and high purity (particularly with regard to alumina and silica impurities). They were deposited at two different thicknesses (375 and 1100 μm). Some of the specimens had dense vertically cracked (DVC) inner layers. The two-layer TBC microstructure was prepared by adjusting the spraying parameters during deposition.

In the testing of TBCs, a bottom loading furnace was used to cyclically oxidize the TBC specimens. In this test, the specimens were heated to the test temperature, usually 1373 K (1100 °C), in 10 minutes. The specimens were held at the test temperature for 45 minutes and then cooled to about 373 K (100 °C) in 10 minutes. The 15-hour cycles as well as pseudo-isothermal tests were also performed in a bottom loading furnace (The pseudo-isothermal test is similar to the FCT, except the 45-minute hold at 1373 K (1100 °C) is replaced by a 60-hour hold). The 10-minute cycles were performed in a vertical tube furnace, which contained a large thermal mass to permit rapid specimen heating and which had a high velocity air blower to permit rapid specimen cooling. Each rapid cycle consisted of heating to 1373 K (1100 °C) in 2.5 minutes, holding at 1373 K (1100 °C) for 5 minutes, and cooling to 303 K (30 °C) in 2.5 minutes. The visual examination of the specimens was done periodically to check for any signs of failure. Macrographs showing typical failures for EBPVD TBCs are given in Figure 12.

JETS testing[17] was also used in testing of some of the APS TBC coated systems. In this test, disk specimens are loaded onto a large rotating ring and rotated through a series of different positions. In the first position, the specimen is rotated under an oxy-propylene flame for 20 seconds, which heats the topcoat surface to approximately 1673 K (1400 °C), while the backside of the superalloy only reaches temperatures of 1123 K to 1173 K (850 °C to 900 °C). The specimen is then rotated under a nozzle that cools the YSZ surface for another

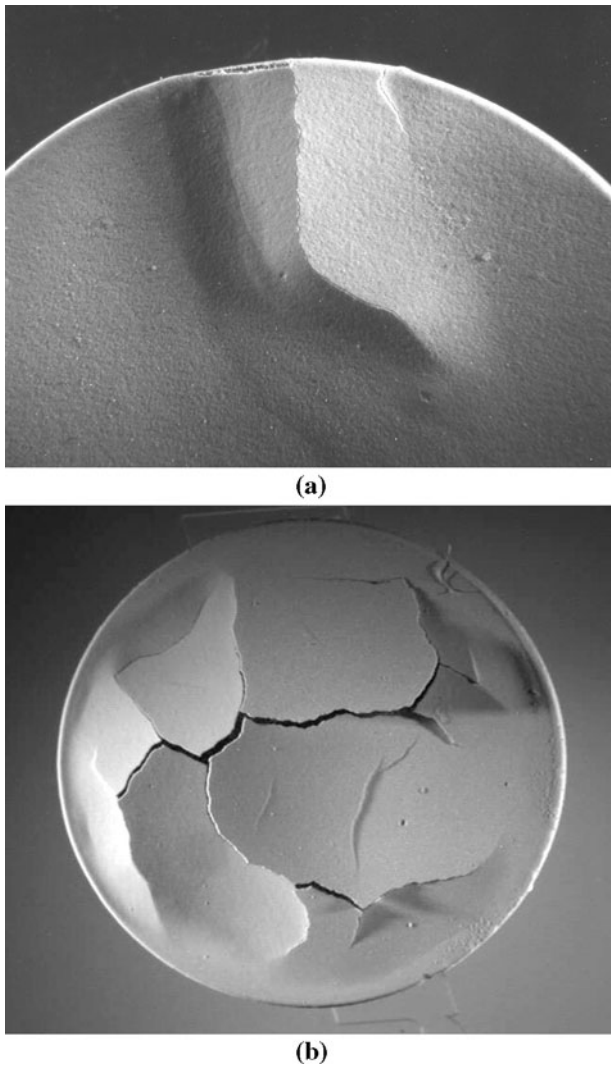

Fig. 12—Micrographs showing typical failures for EBPVD TBCs. (*a*) At times, the failures initiate at specimen edges, and (*b*) other failures involve buckling in the center of the coupon.

20 seconds with compressed nitrogen. After this, the specimen is rotated to positions where it undergoes ambient air cooling for two periods of 20 seconds each, and then the heating step is repeated.

The failed TBCs were examined using optical metallography and scanning electron microscopy (SEM). These examinations were performed on the surfaces exposed by the failures as well as by preparing cross sections using conventional metallographic techniques.

III. RESULTS

A. *TBC Failures*

A substantial number of articles have addressed TBC failures, and failure mechanisms have been proposed. As discussed by Evans *et al.*,[19] it is useful to distinguish between extrinsic and intrinsic TBC failures. The extrinsic category includes damage induced by particle impact and delaminations arising from penetration into the

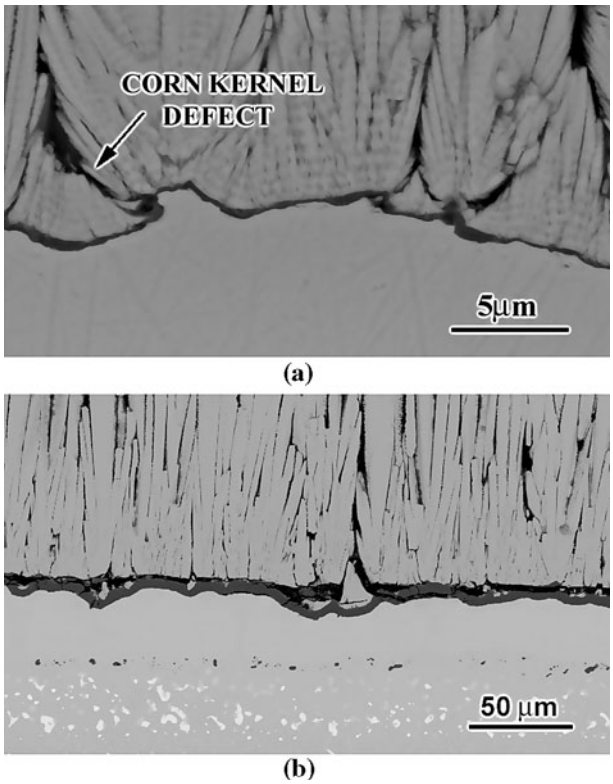

Fig. 13—Scanning electron micrograph of a typical heavy grit blasted TBC system with Pt aluminide bond coat with corn kernel TBC defects (*a*) in the as-processed condition and (*b*) after failure.

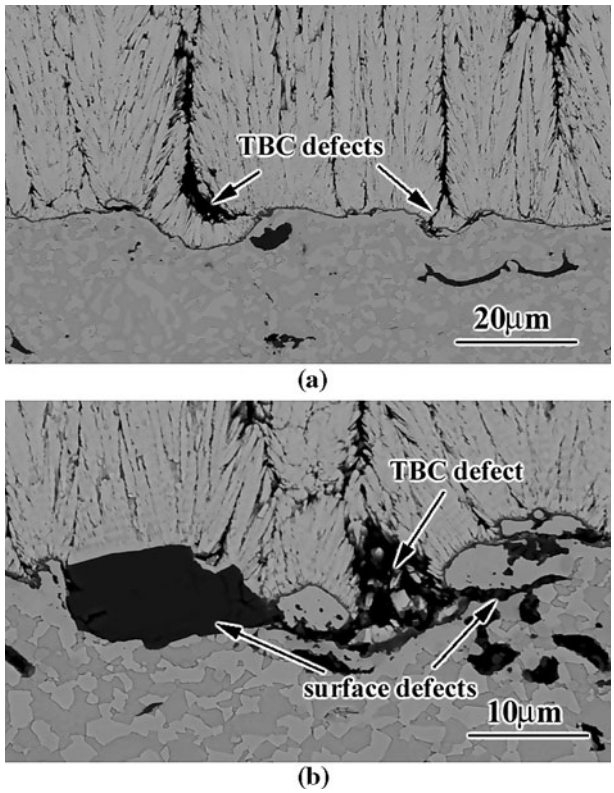

Fig. 14—Scanning electron micrographs showing the typical state-of-the-art TBC systems with NiCoCrAlY bond coats in the as-processed condition. Defects were present, such as (*a*) TBC defects (corn kernels) and (*b*) surface defects.

TBC of deposits of calcium-magnesium-alumino-silicate (CMAS), whereas the intrinsic category involves mechanisms that arise because of strain misfit associated with the constituent materials. This article will consider only intrinsic failure mechanisms.

In discussing intrinsic TBC failures, it is necessary to distinguish between TBCs fabricated *via* EBPVD and APS as well as the two different bond coats, namely, platinum-modified aluminide and MCrAlY coatings. However, in the case of APS TBCs, platinum aluminide bond coats are not used.

In this study, heavy grit-blasted Pt aluminide coatings with EBPVD TBCs subjected to 1-hour thermal cycles failed by the ratcheting mechanism. Figure 13 presents such a system in the as-processed condition and after failure. The interface became highly irregular, eventually causing failure. NiCoCrAlY coatings failed as a combined result of TGO growth and defects that were identified as TBC defects, transient oxides, surface defects, and reactive element-rich oxide protrusions. Examples of some of the defects are shown in the micrographs of as-processed coatings given in Figure 14. The details of the failure mechanisms for these two systems were discussed in an earlier publication.[18]

Some work also has been done on no bond coat systems for EBPVD TBCs on Renè N5 substrates. A summary of cyclic lives of the various specimens is presented in Table I along with the average lives of the improved systems that will be described next in this article. It can be seen that some of the no bond coat

Table I. Comparison of EBPVD YSZ TBC Failure Lives on No Bond Coat and Pt-Modified N5 to Optimized Platinum Modified Aluminide and NiCoCrAlY Bond Coats

Type Specimen	Failure Time at 1373 K (1100 °C) (Number of 1-Hour Cycles to Failure)
N5 (first lot) grit blast and preoxidation	140, 1280, 700+
N5 (second lot) grit blast	1580, 4100, 1840+, 3660+
N5-Pt overlayer (first lot) grit blast, Pt layer + anneal, grit blast, preoxidation	500, 660
N5-Pt overlayer (second lot) grit blast, Pt layer + anneal	2300+, 7130+
Optimized platinum modified aluminide bond coat (average of 9 specimens; one did not fail after 3780 cycles)	2040
Optimized NiCoCrAlY bond coat (average of 9 specimens; one did not fail after 1520 cycles)	956

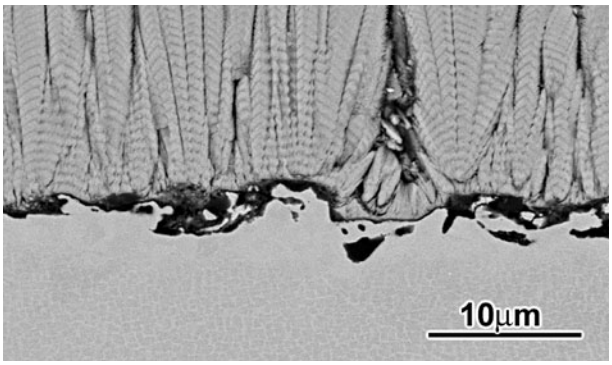

Fig. 15—Scanning electron micrograph of as-processed EBPVD on Renè N5. The TBC-N5 substrate interface is irregular and corn kernel defects are evident in the TBC at the TBC-alloy interface.

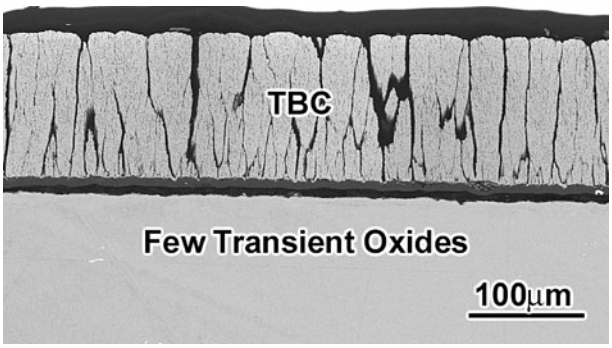

Fig. 16—Scanning electron micrograph of failed EBPVD YSZ TBC (second lot) on Renè N5 after 4100 cycles at 1373 K (1100 °C).

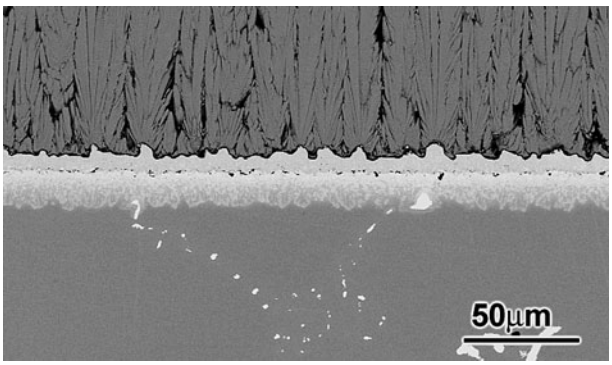

Fig. 17—Scanning electron micrograph of an as-processed EBPVD YSZ TBC on Renè N5 with a Pt overlayer.

systems have surprisingly competitive TBC lives. An as-processed no bond coat TBC is presented in Figure 15. The TBC/superalloy interface is irregular and oxides are evident along this interface. A failure of such a no bond coat system is presented in Figure 16, and it is apparent that failure has occurred along the TGO/superalloy interface, but no rumpling or ratcheting has occurred. An as-processed TBC on Renè N5 with a diffused platinum layer is presented in Figure 17. The interface between the TBC and the substrate is irregular due to the electrolytic process used to deposit the platinum. The TBC on this type of bond coat did not fail after 7000 cycles, and a cross section of this

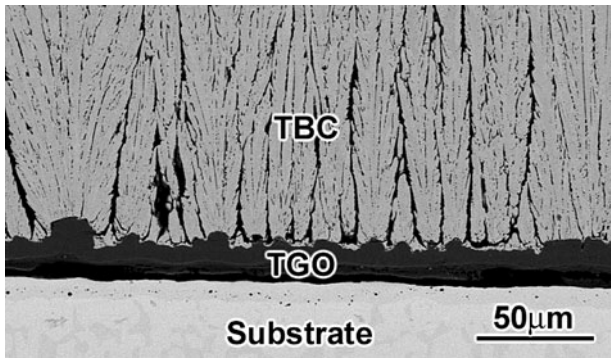

Fig. 18—Scanning electron micrograph of an EBPVD YSZ TBC on Renè N5 with a platinum overlayer. This specimen did not fail after ~7000 cycles of oxidation at 1373 K (1100 °C). (The TGO separated from the coating during metallographic preparation).

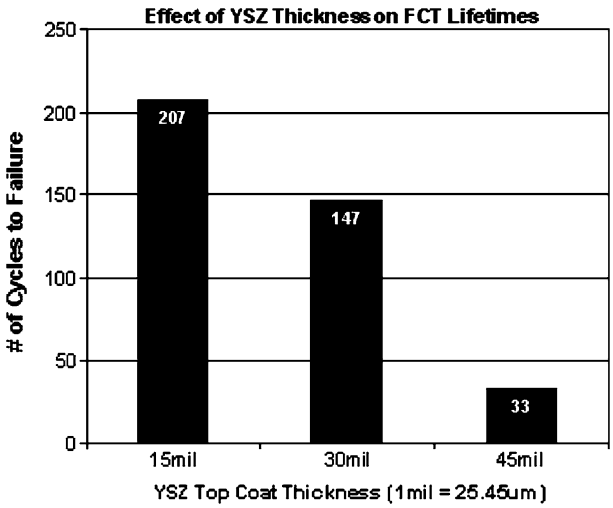

Fig. 19—Number of cycles to failure for APS YSZ TBCs with NiCoCrAlY bond coats and varying TBC thicknesses, cyclically exposed at 1373 K (1100 °C).

specimen is presented in Figure 18. The TGO shows no indications of rumpling or ratcheting.

It has been found that the lives of APS TBC coated NiCoCrAlY coatings are strongly influenced by TBC thicknesses (Figure 19). Moreover, the failure modes can differ between thick and thin TBCs. For thick TBC (*e.g.*, 1125 μm), the failure is well into the TBC at splat boundaries (Figure 20(a)). As the TBC thickness is decreased, the failure moves toward the TBC/TGO interface and the failure mechanism is similar to that described previously for such TBC systems (Figure 20(b)). It has been found that APS TBC failures on NiCoCrAlY bond coats are also influenced by the alloy substrate (Figure 21).[20]

B. *Improved TBCs*

Among various modifications made to EBPVD TBC coated NiCoCrAlY bond coatings, Pt overlayer and the surface polishing resulted in the most significant improvements. For example, the average life for the

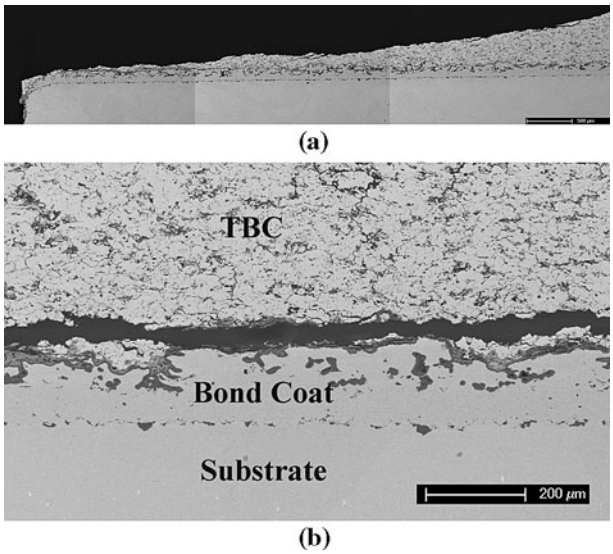

Fig. 20—(*a*) In the case of thick (>1000 μm) APS TBCs, failure occurred in the TBC where the initial cracking initiated at the specimen edge. (*b*) For thinner thicknesses, the failure was along the TBC-TGO interface.

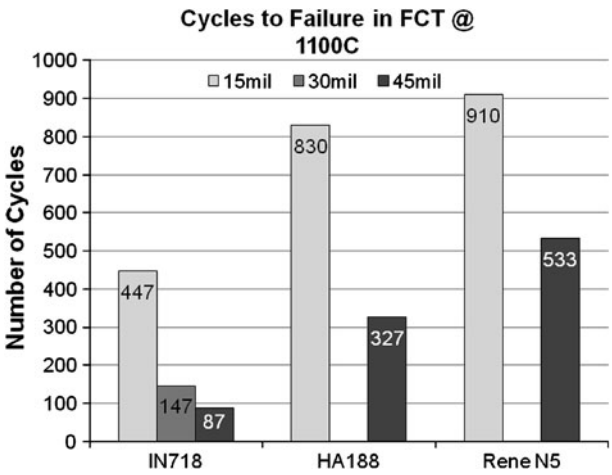

Fig. 21—Cycles to failure in a cyclic oxidation test at 1373 K (1100 °C) for APS YSZ TBCs on NiCoCrAlY bond coats with different TBC thicknesses on three different alloy substrates.

NiCoCrAlY bond coat with the Pt overlayer was 1080 cycles (average of five specimens), whereas the average life of the state-of-the-art specimens was 72 cycles (average of ten specimens).The as-processed TBC on the polished NiCoCrAlY bond coat (Figure 22), was quite smooth, and the system was free from defects. The as-processed system with the NiCoCrAlY bond coat with the platinum overlayer (Figure 23) had a very nonuniform TBC/bond coat interface. The bond coat contained platinum in the coating adjacent to the TBC. The cyclic oxidation results for these two modified systems are compared to the state-of-the-art system in Figure 24. Both modifications have improved the cyclic oxidation life of this TBC system. A micrograph of the polished bond coat after exposure is presented in

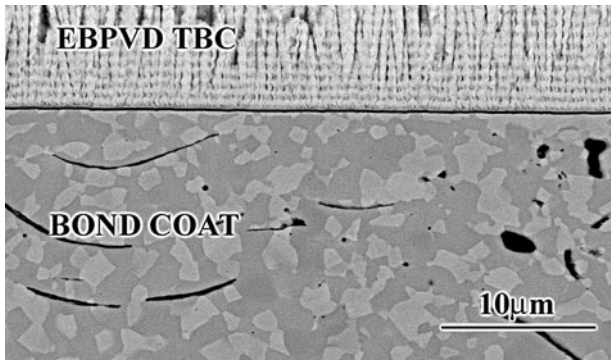

Fig. 22—Micrograph showing as-processed TBC on polished NiCoCrAlY bond coat. The TBC-TGO interface is very smooth and no defects are evident.

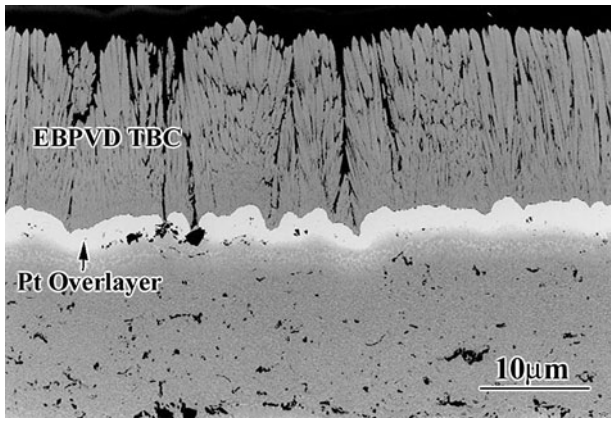

Fig. 23—Scanning micrograph of an as-processed NiCoCrAlY bond coat with a platinum overlayer.

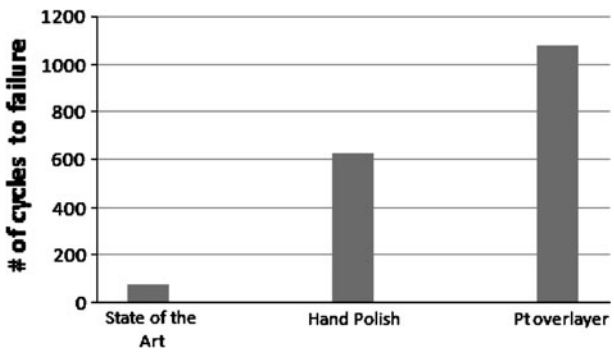

Fig. 24—Average failure times for TBC systems with modified NiCoCrAlY bond coats that were exposed to cyclic oxidation at 1373 K (1100 °C).

Figure 25. The TGO is thick due to reactive element oxides in the TGO, but the TBC/TGO interface is very smooth and free from most of the defects. The TBC system with the NiCoCrAlY bond coat with the Pt overlayer is presented in Figure 26. Cracks are evident in the TBC. The growth rate of the TGO is slower compared to the growth rate of the TGO on the state-of-the-art NiCoCrAlY systems (Figure 27).

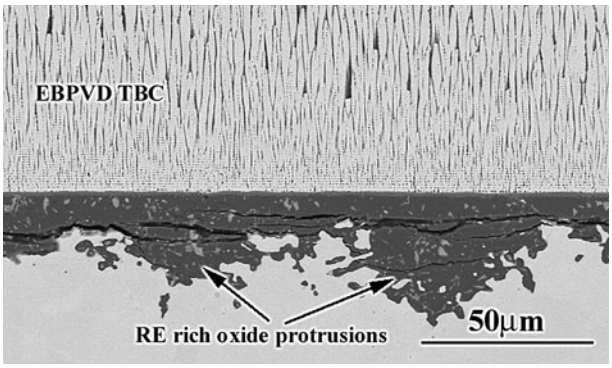

Fig. 25—Scanning electron micrograph of a TBC with a hand-polished NiCoCrAlY bond coat after 1520 cycles of exposure at 1373 K (1100 °C).

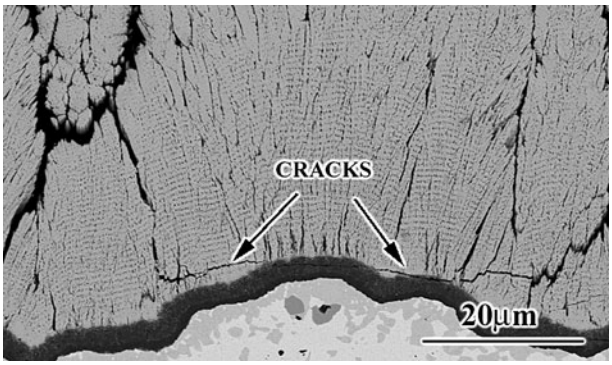

Fig. 26—Scanning electron micrograph of TBC on NiCoCrAlY with Pt overlayer after cyclic oxidation exposure at 1373 K (1100 °C).

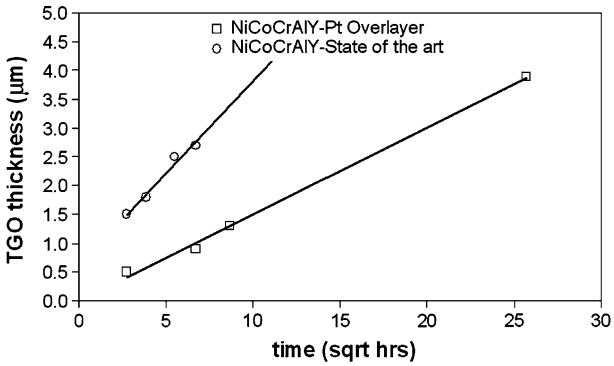

Fig. 27—TGO thickness *vs* square root of time for an EBPVD YSZ TBC with a Pt overlayer on a NiCoCrAlY bond coat and for a state-of-the-art NiCoCrAlY bond coat at 1373 K (1100 °C).

Surface condition also had a significant improvement in the lives of EBPVD TBCs on Pt aluminide coatings. An as-processed TBC with a light grit-blasted bond coat is presented in Figure 28. Few defects are evident and a TBC system with such a bond coat finish did not fail after 8000 cycles at 1373 K (1100 °C) (Figure 29).

In the case of APS TBC coated NiCoCrAlY coatings, use of dense vertically cracked (DVC) inner layers in the top coat showed some promising results. The microstructure of such a TBC in the as-processed condition is presented in Figure 30. The inner DVC layer is dense

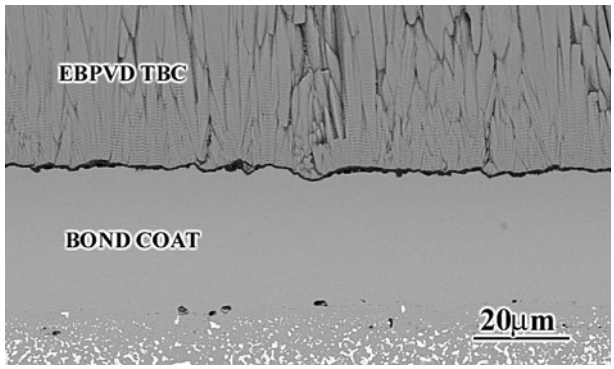

Fig. 28—Scanning electron micrograph of a typical TBC system with light grit blasted Pt aluminide bond coat in the as-processed condition showing the relatively smooth interface compared to the interfaces of heavy grit blasted Pt aluminide bond coats.

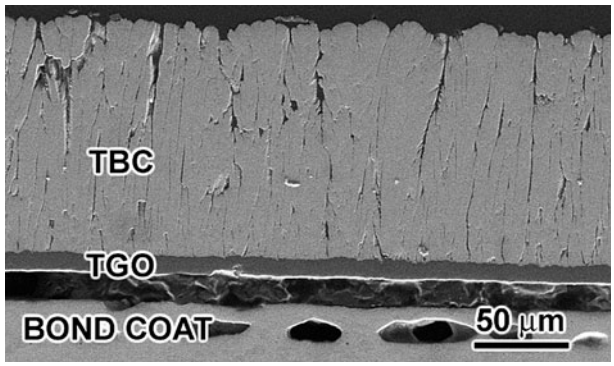

Fig. 29—Cross-sectional view of TBC on light grit blasted Pt aluminide bond coat. This TBC did not fail after 8000 cycles at 1373 K (1100 °C). Voids formed in the bond coat as a result of interdiffusion (the TGO detached from the bond coat during metallographic preparation).

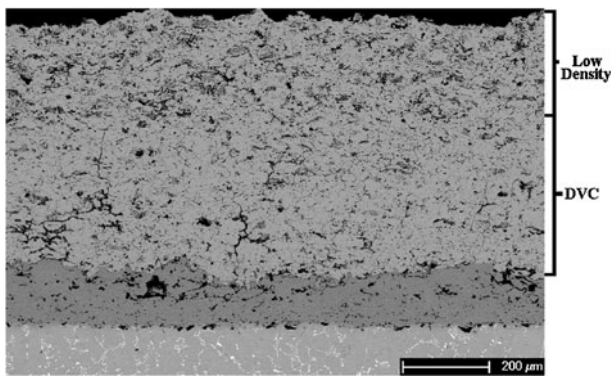

Fig. 30—Cross-sectional micrograph of an APS TBC system with DVC inner layers in the as-processed condition.

with vertical cracks and the upper layer is more porous. This type of microstructure is obtained by adjusting spraying parameters during deposition. Cracking was sometimes observed at the interface between the two layers of the TBC. Even though specimens without DVC layers for direct comparison were not available due to different substrates used, similar cyclic lives of systems

with thin (375 μm) and thick TBCs (1100 μm) with DVC layers (~600 cycles at 1373 K (1100 °C)) suggested improvement in the presence of DVC layers.

C. *Effect of Exposure Conditions*

All of the results described previously for both state-of-the-art and improved TBCs were obtained under identical test conditions: exposure in air at 1373 K (1100 °C) in a bottom loading furnace using 1-hour cycles. The lives of TBCs show a strong temperature dependence, and in some cases, the spallation lives and failure mechanisms vary with the type of thermal exposure.

1. *Effect of temperature*

Table II shows the effect of temperature on the failure for state-of-the-art EBPVD TBCs with NiCoCrAlY and Pt-aluminide bond coats exposed using 1-hour cycles in a bottom loading furnace. The number of cycles to failure decreases markedly with increasing exposure temperature (approximately a factor of 10 for each 100 K (100 °C) increase). An Arrhenius plot of these data[18] yielded an apparent activation energy of 356 kJ/mole, which is quite close to that for the parabolic rate constant for the growth of α-alumina.

2. *Effect of cycle frequency*

The effect of cycle frequency on the failure of EBPVD TBCs was found to differ for systems with NiCoCrAlY and Pt-aluminide bond coats.[21] Table III presents data for the effect of cycle frequency on both the number of cycles to failure and the hot time to failure of state-of-the-art EBPVD TBCs with NiCoCrAlY and Pt-aluminide bond coats. Approximate results for the hot time of exposure under the isothermal condition, which will result in spallation during cooling, are included. Table III indicates the hot time to failure of TBCs with Pt-aluminide bond coats decreases markedly as the cycle frequency is increased. Figure 31 indicates that the hot time to failure decreases linearly with the logarithm of the cycle length. The life of TBCs with NiCoCrAlY bond coats is rather insensitive to cycle frequency and actually increases for the rapid, 10-minute cycles.

The microstructures of the failed specimens are also different for the two bond coats. Figure 32 shows that the fracture occurs mainly along the TGO/bond coat interface for the NiCoCrAlY bond coat regardless of cycle frequency. There is no evidence of rumpling for this bond coat. (Shi *et al.*[22] reported rumpling for NiCoCrAlY bond coats when the cyclic exposures are carried out with a temperature gradient across the specimen.) Figure 33 indicates that the failure for Pt-aluminide bond coats occurs along the TGO/bond coat interface for isothermal exposures and by a ratcheting mechanism for 1-hour cycles (as described previously). The 15-hour cycles result in a mixed fracture surface, but much of the failure proceeds along the TGO/bond interface. The fracture surface for the rapidly cycled specimens actually shows more exposed bond coat than that for the 1-hour cycles. This is the result of profuse void formation in these coatings, as illustrated in Figure 34.

The effect of cycle frequency was apparent on the hot time to failure for APS TBCs subjected to different thermal tests. The hot time to failure for identical 350 to 1100 μm APS TBCs on argon-shrouded NiCoCrAlY bond coats with IN718 substrates that were thermally cycled in two different tests, the FCT and the pseudo-isothermal tests, is shown in Figure 35. In each of these

Table II. Effect of Exposure Temperature on the Cycles to Failure of State-of-the-Art EBPVD TBCs with NiCoCrAlY and Pt-Aluminide Bond Coats (the Number of Specimens Tested is Given in Parentheses)

Temperature, K (°C)	NiCoCrAlY	Pt-Aluminide
1273 (1000)	670 (2)	—
1373 (1100)	70 (10)	1118 (8)
1473 (1200)	7 (2)	128 (3)

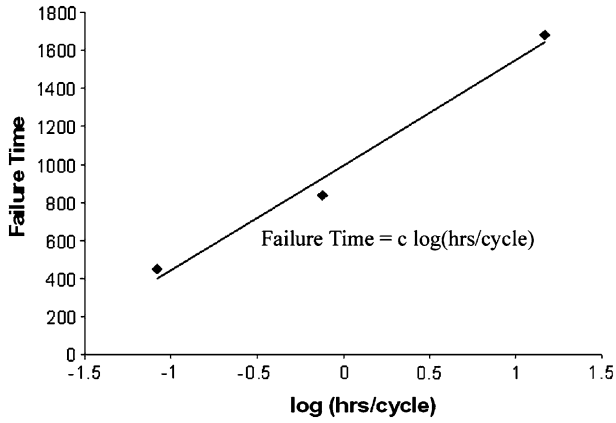

Fig. 31—Failure times for EBPVD YSZ TBCs on platinum aluminide bond coats for cyclic oxidation at 1373 K (1100 °C) as a function of cycle length.

Table III. Effect of Cycle Frequency on the Cycles to Failure and Hot Time (Hours) to Failure of State-of-the-Art EBPVD TBCs with NiCoCrAlY and Pt-Aluminide Bond Coats Exposed at 1373 K (1100 °C) (the Number of Specimens Tested is Given in Parentheses)

	NiCoCrAlY		Pt-Aluminide	
Cycle Frequency	Cycles	Hot Time	Cycles	Hot Time
Isothermal	—	50 (4)	—	>1000 (3)
15-h cycles	2 (1)	30 (1)	112 (2)	1680 (2)
1-h cycles	70 (10)	53 (10)	1118 (8)	839 (8)
10-min cycles	5785 (2)	483 (2)	5422 (2)	452 (2)

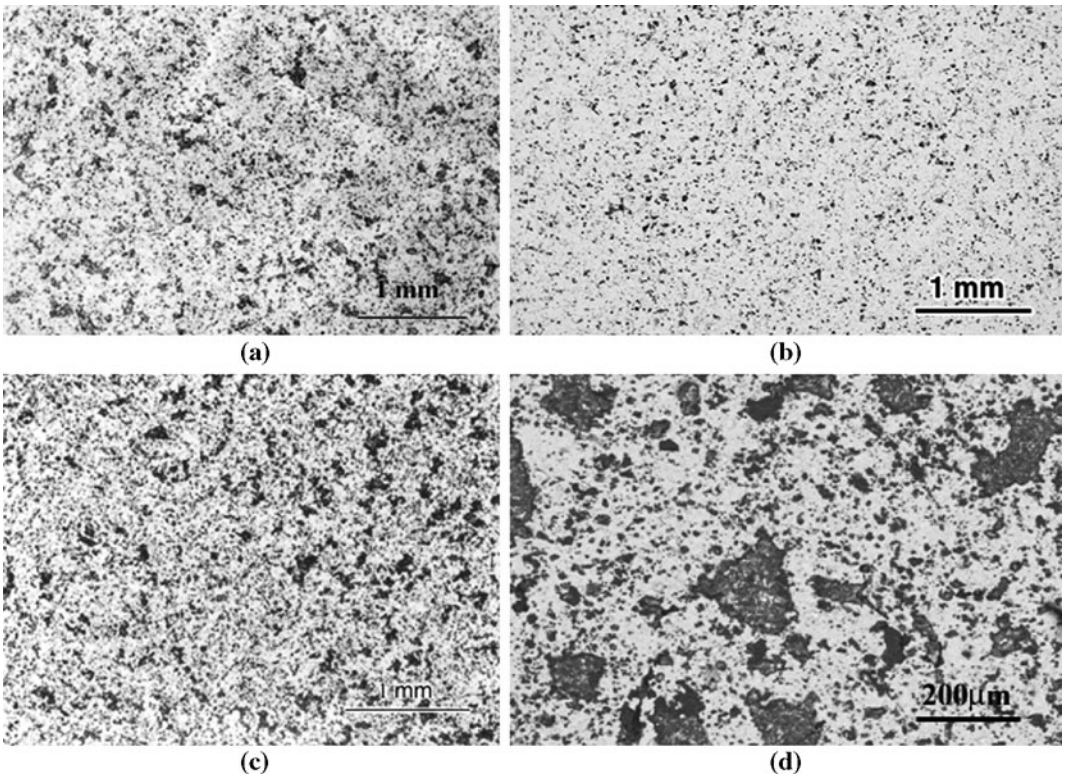

Fig. 32—Scanning electron micrographs showing NiCoCrAlY bond coat surfaces after spalling of EBPVD YSZ TBCs after cyclic oxidation at 1373 K (1100 °C), where cycle length is varied. (*a*) 100-h isothermal cycle (1 cy), (*b*) 15-h cycles (2 cy), (*c*) 1-h cycle (102 cy), and (*d*) rapid cycles (8419 cycles).

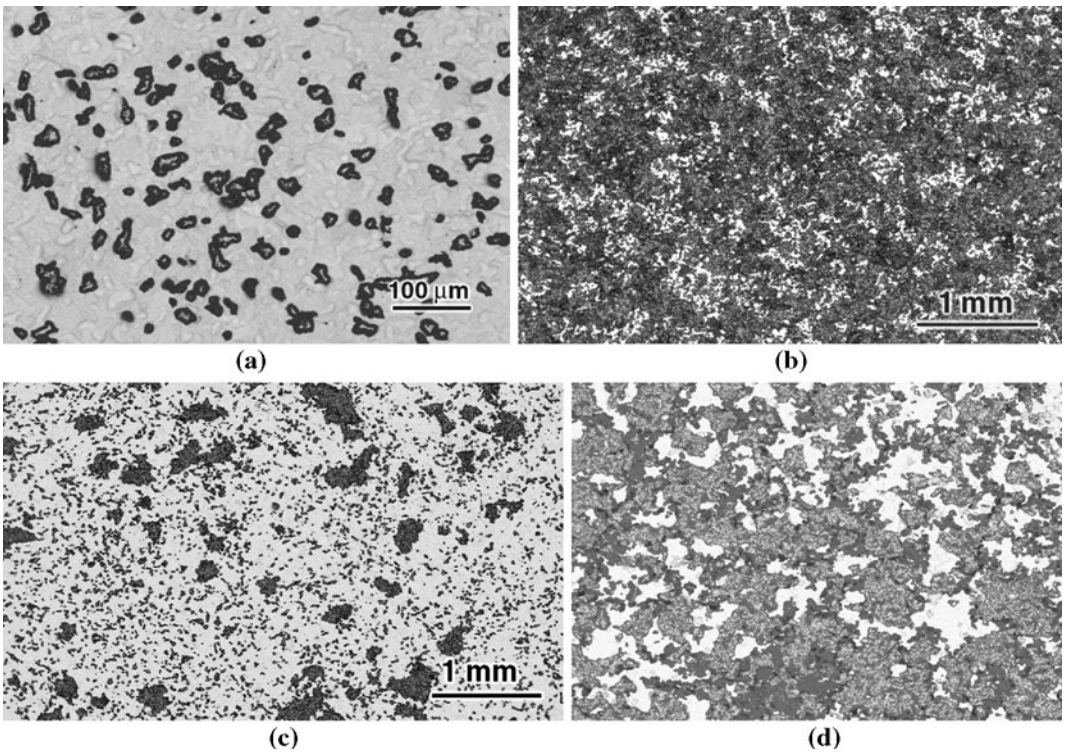

Fig. 33—Fracture surface exposed upon failure of EBPVD YSZ TBCs on platinum aluminide bond coats in cyclic oxidation for different cycle lengths and temperatures. (*a*) 100-h isothermal (1473 K (1200 °C), 1 cy), (*b*) 15-h cycles (1373 K (1100 °C), 88 cy), (*c*) 1-h cycles (1473 K (1200 °C), 120 cy), and (*d*) rapid cycles (1373 K (1100 °C), 6556 cycles).

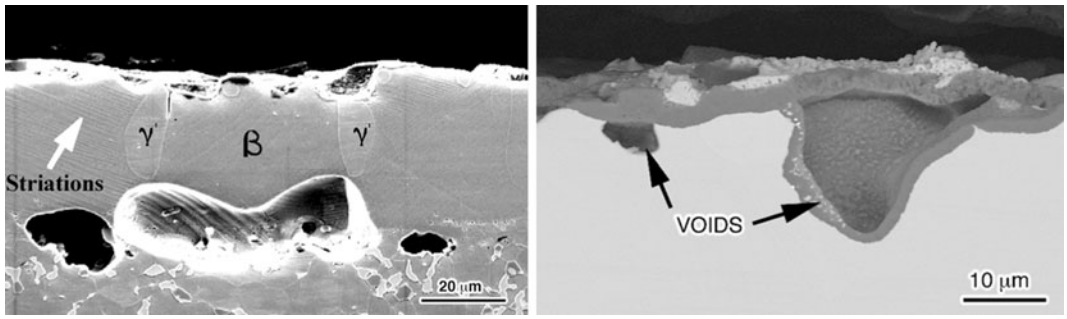

Fig. 34—Scanning electron micrographs showing voids that develop in platinum aluminide bond coats after rapid cycling at 1373 K (1100 °C).

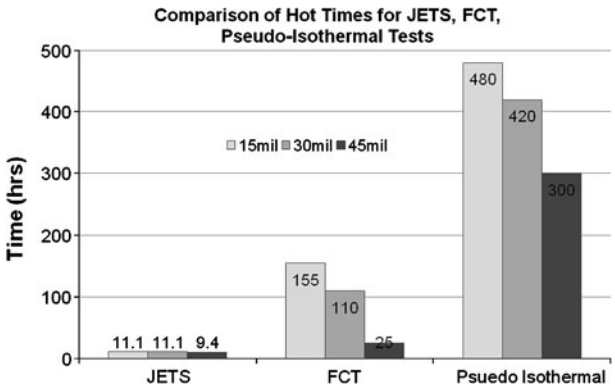

Fig. 35—Comparison of hot times for JETS, FCT, and pseudo-isothermal tests of IN718-NiCoCrAlY-APS TBC systems (1 mil = 25.45 μm) with different YSZ TBC thicknesses.

tests, the heating and cooling periods were identical so the only difference in the temperature-time profiles was the length of the isothermal hold at 1373 K (1100 °C). As shown by the graph, the hot time to failure was increased by reducing the number of heating and cooling periods (*i.e.*, switching from FCT testing to pseudo-isothermal testing). Furthermore, the JETS test, which has the most rapid cycling (20 seconds heating, 20 seconds cooling, and 40 seconds ambient cooling), had the shortest hot time to failure, followed by the FCT test, and then the pseudo-isothermal test. However, it should be noted that the JETS test induces a thermal gradient over the TBC, which is different from the other two tests, so another factor besides thermal cycle frequency may be involved here. Nonetheless, comparison of only the FCT and pseudo-isothermal testing results indicates the presence of a thermal cycle frequency effect.

3. *Effect of thermal gradients*

The failures of TBCs can also differ depending on whether the entire specimen (substrate, BC, and topcoat) is heated to a uniform temperature, as in the furnace cyclic test FCT, or exposed under a thermal gradient.

Figure 35 compares the hot time and cycles to failure of the porous APS TBCs on IN 718 substrates (*i.e.*, those in Figure 20) in three different tests: JETS, FCT, and a "pseudo-isothermal test." The hot time to failure in all three tests is reduced as the topcoat thickness is increased. Also, for a given topcoat thickness, the number of cycles to failure increases but the hot time to failure decreases as the cycle frequency of the test increases.

Figure 36 compares the fracture surfaces of the thickest (1.1 mm) topcoats in the three tests. Figure 36(a) corresponds to the cross section in Figure 20(a) for the FCT, and the surface appears to be comprised entirely of YSZ. The fracture surface of the specimen failed in the pseudo-isothermal test (Figure 36(b)) is similar to that for the FCT, except there is somewhat less YSZ remaining on the surface. The fracture surface of the FCT was completely covered by YSZ with very minimal amounts of TGO showing, whereas the surface of the pseudo-isothermal specimen was comprised of 75 pct YSZ and 25 pct TGO and bond coat. The JETS specimen failed by the spallation of portions of the YSZ top coat, which left a dimpled morphology at the fracture surface, as seen in Figure 36(c). The darker rim around the edge of the button shows an edge crack fully surrounded the button early in the test. The dark tint is caused by carbon deposited by the JETS flame, which has decorated the extent of the inward growth of the edge crack. The inward growth varied from about 1000 to 3000 μm at different locations around the circumference. Finally the YSZ layer completely spalled at the end of the test on final cooldown, since no carbon deposit is seen in the central area of the button. Each of the specimens examined contained roughly 40 dimples. The individual dimples had a raised outer YSZ edge, a flat YSZ/TGO inner ring, and occasionally a raised center YSZ peak. The average diameter of the dimples was 3.3 mm with a standard deviation of 0.5 mm. Given this statistic, the average number of dimples across the diameter of a single button is approximately seven to eight dimples. SEM analysis of the fracture surface revealed that fracture occurred mostly within the YSZ top coat, because there was relatively little TGO at the fracture surface. The fracture path appeared to be mixed between intersplat fracture and intrasplat fracture. Examination of thinner topcoats, which were in an earlier stage of degradation, indicated that the dimpled failure in the JETS test involved formation of horizontal cracks in the lower portion of the topcoat, followed by the formation of vertical cracks and finally linking of the horizontal and vertical cracks to remove a portion of the topcoat.

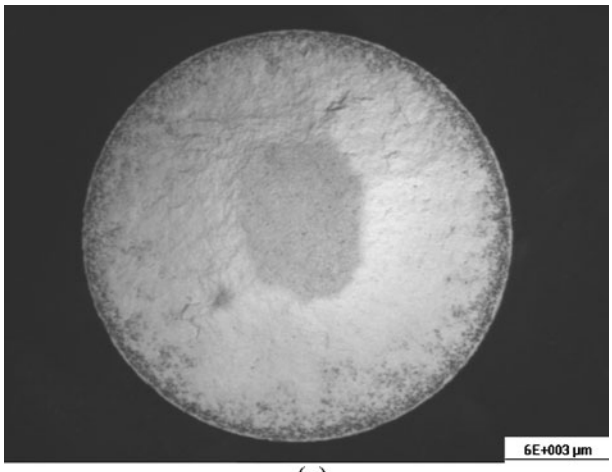

(a)

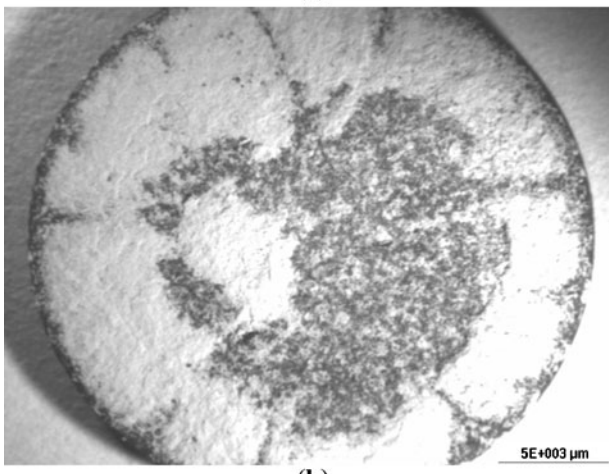

(b)

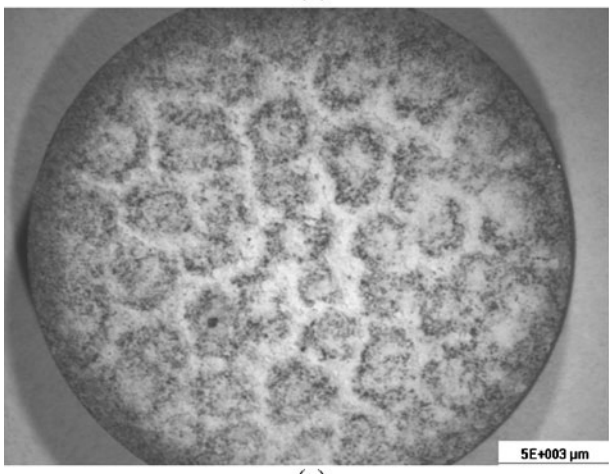

(c)

Fig. 36—Comparison of the fracture surfaces of TBC specimens with a 1.1-mm-thick topcoat and IN718 substrate after failure in (*a*) a furnace cycling test, (*b*) a pseudo-isothermal test, and (*c*) a JETS test.

IV. DISCUSSION

A. *TBC Failures*

Considering the failures for the various TBCs discussed in Sections III–A of this article, the schematic shown in Figure 37 is presented in order to attempt to provide a qualitative description applicable to all of these failures. Defects may be present in the TBC system, and if not, cracks will eventually develop upon exposure at elevated temperatures coupled with thermal cycling. The important factors are the stored energy in the TGO and TBC due to growth of the TGO, phase transformations in the bond coat, and thermal cycling of the TBC system coupled with bond coat deformation, sintering of the TBC, TGO relaxation, and TBC fracture toughness. Cracks, once formed, propagate and coalesce until failure occurs.

The results obtained with the no bond coat TBC specimens also show that bond coat strength is an important parameter. Both the aluminide and overlay bond coats can be easily deformed at temperatures above 1273 K (1000 °C), and TBC lives on these two bond coats may be improved by making modifications to increase their high-temperature strengths.

It has been found that the superalloy substrate also affects the lives of TBCs.[20] A good correlation was shown between the cyclic life of the APS TBC and TBC/substrate CTE mismatch (Figure 38). The magnitude of the CTE mismatch between the superalloy substrate and top coat will affect the elastic strain energy stored in the topcoat during cooling from the exposure temperature. Larger strain energies will lead to shortened spallation lives. The superalloy substrate also affects the lives of TBCs *via* diffusion of elements from the superalloy into the bond coats. The effects of this interdiffusion may cause TBC lives to be increased or decreased depending upon the particular element. For example, when Hf diffuses into the bond coat the adherence of the TGO can be improved, which can result in longer TBC lives. On the other hand, the diffusion of tantalum into the bond coat can affect the composition of the TGO such that oxides other than alumina form in the TGO. Such a condition can adversely affect the lives of the TBC.

Based on the furnace cyclic test data available so far, APS TBC systems with NiCoCrAlY coatings outperformed EBPVD TBC systems with NiCoCrAlY coatings, when both were applied to N5 substrates. The average failure times were around 900 cycles for the APS TBC coated systems, whereas it was around 100 cycles for the EBPVD TBC systems. Moreover, the APS TBCs were thicker than EBPVD TBCs (375 *vs* 125 μm, respectively). Some variation was present in the cyclic lives of EBPVD TBCs, whereas the cyclic life results were very reproducible in the case of APS TBCs. This might be due to the fact that EBPVD TBC systems tested so far were more prone to failure in the presence of defects than APS TBC systems. The adherence between bond coat/TGO/TBC might be stronger in the case of APS TBC systems, so that the cracks initiated in the vicinity of defects do not propagate to failure. For example, the APS TBC coated systems did not fail despite cracks that were observed as early as 25 pct of their lifetime. More work needs to be done for direct comparison of the adherence in these systems. It would also be useful if comparison is made under JETS testing conditions, since FCT is a more severe test for EBPVD TBCs than APS TBCs.[17]

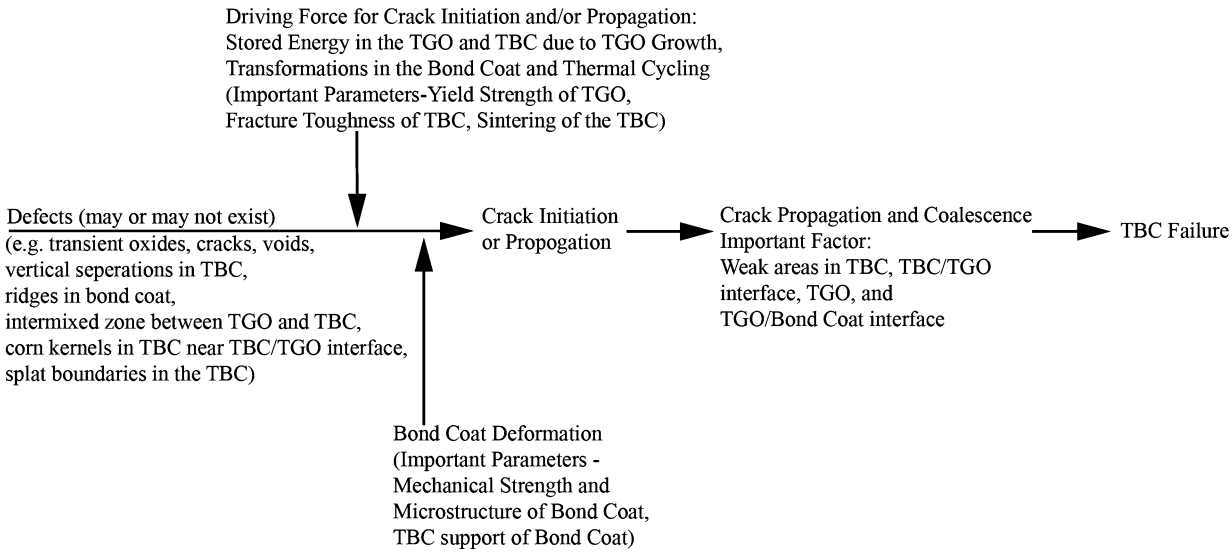

Fig. 37—Sequential diagram showing qualitatively the factors that can affect TBC failure.

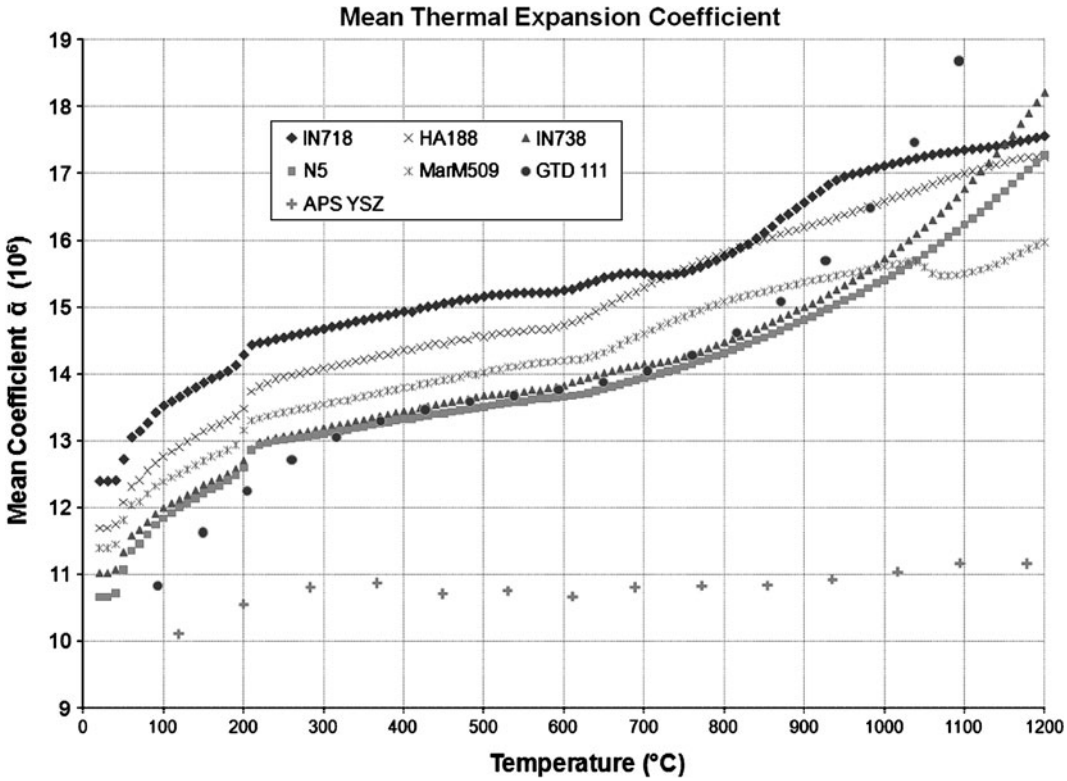

Fig. 38—Coefficients of thermal expansion for some relevant alloys as a function of temperature.

B. *Improved TBCs*

The failure of the EBPVD TBCs on both bond coats is very susceptible to defects, and TBC lives increase as defects are minimized. Bond coat oxidation is a very important factor in determining TBC lives. More transient oxidation takes place for NiCoCrAlY bond coats compared to platinum aluminide bond coats, but such transient oxidation of the NiCoCrAlY bond coats can be minimized by polishing the bond coat or by enriching the bond coat surface with platinum. It is believed that the increased life of the EBPVD TBC is due to improved adherence and the development of pure and slow growing TGO on the platinum-coated NiCoCrAlY. In the case of hand-polished specimens, the improved lives were attributed mainly to the lack of defects along the TGO/TBC interface (mainly TBC defects and transient oxides).

Since rough surfaces are conducive to bond coat rumpling because defects exist in the TBC that permit the bond coat to recede, a light grit blast was used on Pt

aluminide coatings to attempt to produce a TBC system with fewer of these defects. Significant improvements in lives were observed, which are attributed to the inhibition of the ratcheting type of failure.

Based on testing of APS TBCs with different thicknesses, the trend was that thick TBCs failed after significantly shorter exposure times than thin TBCs. However, similar and relatively longer cyclic lives of thin and thick APS TBCs with DVC layers suggested that the presence of inner DVC layers provide some strain relief preventing early failure of thick TBCs in the lower portion of the TBC, where failure usually takes place. Improvement in lives despite the presence of some cracking observed along the interface between lower and upper TBC layers indicates the possibility of further improvements by better controlling the spraying parameters.

C. *Effect of Exposure Conditions*

1. *Effect of temperature*

The Arrhenius relationship between the failure time of EBPVD TBCs and temperature, which gives an activation energy that is close to that of the parabolic rate constant for the growth of α-alumina, suggests a significant role of TGO growth rate on the failure of these TBC systems. Therefore, the stored energy in the TGO is believed to be one of the major driving forces in the failure of these systems.

2. *Effect of cycle frequency*

Increasing the cycle frequency decreased the lives of EBPVD TBCs on Pt aluminide coatings, whereas it increased the lives of EBPVD TBCs with NiCoCrAlY coatings. The decreased lives of Pt aluminide coatings are due to development of voids under rapid cycling conditions. The mechanism for profuse void development for rapid cycled Pt aluminide coatings has not been completely characterized, but it is believed that the large number of cycles produces severe deformation of the bond coat due to the thermal expansion mismatch between bond coat and substrate and the martensitic transformation in the coating, both of which contribute to rumpling for slower cycling. The severe deformation presumably forms the voids by a cavitation process. In the case of NiCoCrAlY coatings, such cavitation was not observed, and it is believed that some kinds of stress relief processes are responsible for the improved lives under rapid cycling conditions.

3. *Effect of thermal gradients*

Exposing under a thermal gradient was observed to have an effect on the failure time as well as the failure mechanism of APS TBC systems. More testing and characterization is required for a better understanding of thermal gradient effects.

V. CONCLUDING REMARKS

The failures of EBPVD and APS TBCs were compared. Such a comparison must be done with care since the thicknesses of APS TBCs are usually much greater than those of EBPVD TBCs (>300 and ~200 μm). The failures of both TBCs very often occur at or near the TBC/TGO or TGO/bond coat interfaces due to the strong influence of oxidation of the bond coats on TBC failure. It has been shown that the oxidation of bond coats with EBPVD TBCs can be influenced by controlling the smoothness of the bond coat or adding platinum to the surface of the bond coat. Polishing of APS TBCs is not practical for APS TBCs, since a rough TBC/bond coat interface is necessary to mechanically bond the TBC to the bond coat.

The APS TBCs are more susceptible to failure out in the TBC away from the TBC/TGO interface due to the presence of splat boundaries in the TBCs.

It is also shown that exposure conditions significantly affect TBC failures, as may be expected, but the failures depend on the bond coats, which respond in different ways.

ACKNOWLEDGMENTS

Financial support of this research by ONR (MURI Contract No. N00014-02-1-0801) and National Energy Technology Laboratory under RDS Contract No. DE-AC26-04NT41817 and TBC specimen preparation by Howmet and GE Aircraft Systems are gratefully acknowledged.

REFERENCES

1. M. Peters, C. Leyens, U. Schulz, and W. Kaysser: *Adv. Eng. Mater.*, 2001, vol. 3 (4), pp. 193–204.
2. N.P. Padture, M. Gell, and E.H. Jordan: *Science*, 2002, vol. 296, pp. 280–84.
3. D.R. Clarke and C.G. Levi: *Ann. Rev. Mater. Res.*, 2003, vol. 33, pp. 383–417.
4. A.G. Evans, D.R. Mumm, J.W. Hutchinson, G.H. Meier, and F.S. Pettit: *Prog. Mater. Res.*, 2001, vol. 46 (5), pp. 505–53.
5. J. Aktaa, K. Sfar, and D. Munz: *Acta Mater.*, 2005, vol. 53 (16), pp. 4399–413.
6. S. Sridharan, L. Xie, E.J. Jordan, M. Gell, and K.S. Murphy: *Mater. Sci. Eng. A*, 2005, vol. A393 (1–2), pp. 51–62.
7. I.T. Spitzberg, D.R. Mumm, and A.G. Evans: *Mater. Sci. Eng. A*, 2005, vol. A394 (1–2), pp. 176–91.
8. K.W. Schlichting, N.P. Padture, E.H. Jordan, and M. Gell: *Mater. Sci. Eng. A*, 2003, vol. A342 (1–2), pp. 120–30.
9. A. Rabiei and A.G. Evans: *Acta Mater.*, 2000, vol. 48 (15), pp. 3963–76.
10. J.W. Hutchinson and A.G. Evans: *Surf. Coat. Technol.*, 2002, vol. 149, pp. 179–84.
11. M.Y. He, D.R. Mumm, and A.G. Evans: *Surf. Coat. Technol.*, 2004, vol. 185, pp. 184–93.
12. M. Gell, K. Vaidyanathan, B. Barber, C. Liangtian, and E. Jordan: *Metall. Mater. Trans. A*, 1999, vol. 30A, pp. 427–35.
13. T. Xu, S. Faulhaber, C. Mercer, M. Maloney, and A. Evans: *Acta Mater.*, 2004, vol. 52, pp. 1439–50.
14. R.A. Miller and C.E. Lowell: *Thin Solid Film*, 1982, vol. 95, pp. 265–73.
15. B.C. Wu, E. Chang, S.F. Chang, and C.H. Chao: *Thin Solid Films*, 1989, vol. 172, pp. 185–96.
16. M.Y. He, J.W. Hutchinson, and A.G. Evans: *Mater. Sci. Eng.*, 2003, vol. A345, pp. 172–78.
17. Bolcavage, A. Feuerstein, J. Foster, and P. Moore: *Proc. 22nd Heat Treat/Surface Engineering Conf.*, Indianapolis, IN, Sept. 15–17, 2003, ASM, Materials Park, OH, 2003, pp. 520–29.
18. N.M. Yanar, F.S. Pettit, and G.H. Meier: *Metall. Mater. Trans. A*, 2006, vol. 37A, pp. 1563–80.

19. A.G. Evans, D.R. Clarke, and C.G. Levi: *J. Eur. Ceram. Soc.*, 2008, vol. 28, pp. 1405–19.
20. M.A. Helminiak, N.M. Yanar, F.S. Pettit, T.A. Taylor, and G.H. Meier: *Surf. Coat. Technol.*, 2009, vol. 204, pp. 793–96.
21. G.M. Kim, N.M. Yanar, E.N. Hewitt, F.S. Pettit, and G.H. Meier: *Scripta Mater.*, 2002, vol. 46, pp. 489–95.
22. J. Shi, A.M. Karlsson, B. Baufeld, and M. Bartsch: *Mater. Sci. Eng.*, 2006, vol. A434, pp. 39–52.